Temperature-dependent solid-state reactions with and without Kirkendall effect in Al_2O_3/ZnO, Fe_2O_3/ZnO, and Co_XO_Y/ZnO oxide thin film systems

A. Zolotaryov[1], S. Goetze[2], R. Zierold[1], D. Novikov[3], B. Birajdar[2], D. Hesse[2], and K. Nielsch[1]

1 - Institute of Applied Physics, Jungiusstr. 11, D-20355 Hamburg, Germany
2 - Max Planck Institute of Microstructure Physics, Weinberg 2, D-06120 Halle, Germany
3 – HASYLAB / DESY, Notkestr. 85, D-22603 Hamburg, Germany

Abstract

Temperature-dependent solid-state reactions and the occurrence of the Kirkendall effect are studied in thin film oxide systems applying optical reflection microscopy, X-ray reflectivity, (scanning) transmission electron microscopy, grazing-incidence X-ray diffraction measurements and SQUID magnetometry. The efficiency of the simultaneous application of different analytical methods for the precise selection and investigation of the most interesting samples is demonstrated first on the example of the Al_2O_3/ZnO system, for which the spinel formation after a solid-state reaction and the formation of Kirkendall voids were already reported. The demonstrated methodology is then applied to study Fe_2O_3/ZnO and Co_XO_Y/ZnO film pairs. The investigations clearly demonstrate the temperature-driven formation of a ferromagnetic spinel by a solid state reaction involving the Kirkendall effect in the Fe_2O_3/ZnO system, already after an annealing at 600 °C for one hour. We also report on the solid state reaction in the Co_XO_Y/ZnO system after annealing at 700 °C for one hour, however without the Kirkendall effect and without any evidence of ferromagnetism of the final state.

Introduction

During the last years the interest in processing of porous materials on the nanoscale has drastically increased. It has been stimulated by the successful efforts for controlled fabrication of hollow nanostructures via the Kirkendall effect [1,2]. The Kirkendall effect may occur during interdiffusion orreaction processes, resulting in formation of a porous layer on the side of the more rapidly diffusing component at the interface between two materials with strongly different diffusion coefficients [3].

Recently significant progress has been achieved in the preparation of high-quality thin oxide films via atomic layer deposition (ALD) [4, 5]. This also motivated activities to study the Kirkendall effect in

ALD-grown oxide film pairs during a solid state reaction (SSR) resulting in formation of a spinel oxide. The corresponding reaction can be written as $AO + B_2O_3 \rightarrow AB_2O_4$, where *A* and *B* are elements (metals) with valencies 2^+ and 3^+, respectively, and O is oxygen with a valency of 2^-.

In 2006 a SSR involving the Kirkendall effect has been first reported for ZnO nanowires ALD-covered with Al_2O_3 and subsequently annealed at elevated temperatures [2]. It has been shown that for three-dimensional (3D) Al_2O_3/ZnO nanosystems there is a temperature window between 500 °C and 700 °C in which hollow 3D nanostructures are formed via a solid state reaction involving the Kirkendall effect, without these structures being damaged by re-crystallization effects [6]. Further experiments on planar substrates under ZnO excess have confirmed that the SSR in the Al_2O_3/ZnO system also leads to a $ZnAl_2O_4$ layer formation in the presence of 3D voids [7].

Motivated by the successful studies of the Kirkendall effect in the Al_2O_3/ZnO system there is now a continuous search for ALD oxide pairs in which a SSR involving the Kirkendall effect can be realized. The large number of processing possibilities requires time-effective and reliable analysis procedures for samples in which a SSR and a formation of Kirkendall voids can be rapidly identified and then studied in detail.

In the present study we demonstrate an effective way to identify and precisely analyse solid state reactions and to track the Kirkendall effect in planar thin oxide film systems by combining optical reflection microscopy (ORM), grazing incidence X-ray diffraction (GIXRD), X-Ray reflectivity (XRR), transmission electron microscopy (TEM) and SQUID magnetometry.

We will show that ORM allows fast conclusions on the presence or absence of a SSR in the investigated system already by analysing its light reflection spectrum. A precise phase analysis in the most interesting samples was performed using GIXRD and SQUID magnetometry. It will be shown that the XRR analysis enables the fast selection of those samples in which a formation of Kirkendall

voids is suspected. To provide final evidence of the presence of a SSR and the Kirkendall effect in the previously selected samples, TEM, and STEM/EDX analyses were applied.

The proposed analytical procedure was applied to the Al_2O_3/ZnO system (which is used as a reference) and further to the Fe_2O_3/ZnO and Co_XO_Y/ZnO thin film systems being the primary objects of the current study.

Sample preparation and analysis

The investigated oxide films were deposited using ALD. The ALD process has been implemented on a commercial "Savannah 100" system (Cambridge Nanotech). Commercial Si_3N_4 (100 nm) / Si (001) and SiO_2 (250 nm) / Si (001) wafers were used as substrates. The choice of Si_3N_4 and SiO_2 as buffer materials is justified by their strong thermal stability and inert chemical behaviour in the temperature range applied in this study.

For our research a number of different material pairs were prepared in which the following substances were applied: Al_2O_3, Fe_2O_3, Co_XO_Y and ZnO.

Al_2O_3 and ZnO thin films were deposited at 80 °C using correspondingly the trimethylaluminum (AlMe3, TMA) and diethylzinc (ZnEt2) reaction with water vapour [4]. Both metal-organic precursor sources were maintained at room temperature, whereby the water precursor source was stabilized at 50 °C to obtain a sufficiently high water vapor pressure.

The Fe_2O_3 and Co_XO_Y films were deposited by using a chemical reaction between the metallocene (ferrocene, cobaltocene) and an ozone-oxygen mixture at a chamber temperature of 230 °C [4]. The metallocene precursor source had a temperature of 100 °C whereby the ozone-gas line was at room temperature. All samples for the study were prepared keeping an excess of the ZnO phase relative to the Al_2O_3, Fe_2O_3 and Co_XO_Y films. In addition, an Al_2O_3/Fe_2O_3 film pair was prepared with both films having approximately equal thicknesses.

After the end of the deposition process all samples were divided into pieces which were respectively annealed at 400 °C, 500 °C, 600 °C, 700°, and 800 °C in argon atmosphere for one hour. The remaining sample pieces were used for the analysis of the as-grown films.

The prepared samples were studied using ORM equipped with a digital camera, GIXRD and XRR at the E2 banding magnet beam-line of HASYLAB/DESY with incoming photons flux of 10^8 mm^{-2} and with an energy of the photons of 11.5 keV. TEM and STEM/EDX analyses were performed in a TEM of type Philips CM20T and a STEM of type Philips CM20FEG, respectively, both working at 200 kV acceleration voltage and both equipped with an energy-dispersive X-ray spectrometer (EDX). SQUID data were collected using a commercial MPMS-XL magnetometer (Quantum Design) in the in-plane sample magnetization setup.

Methodology

Below we provide the analysis of the Al_2O_3/ZnO system for which the conditions for a SSR involving the Kirkendall effect were previously reported. The sequence of the provided investigation steps is visualized using the flow diagram in Fig. 1.

ORM was applied as a preliminary step to identify the presence of a SSR. The argumentation here is the following: Thin oxides possess a high transparency in visible light. The white incoming light is reflected and refracted by each layer and each interface correspondingly. The final reflectance spectrum is then sensitive to both the optical properties of the materials and the interfacial roughness. Below it is shown how both factors contribute to the reflectance spectrum of the sample in which a SSR takes place.

In Fig. 2 the ORM images for all as-grown and annealed Al_2O_3/ZnO samples are compared to those for the Al_2O_3/Fe_2O_3 system (and the other systems investigated). It can be seen that for the Al_2O_3/ZnO system a continuous change of the film colour occurs with increasing annealing temperature. The as-grown film shows a gray reflection colour whereas the annealed films change their colours from dark-

yellow towards red-violet. For the Al_2O_3/Fe_2O_3 system there are no colour changes up to a temperature of 700 °C and only small changes of sample colour between 700 °C and 800 °C. The scientific literature supports the fact that the Al_2O_3/Fe_2O_3 system exhibits a high chemical resistance against SSRs far beyond 1000 °C [8]. Any solid state reaction between Al_2O_3 and Fe_2O_3 can be excluded, due to the maximum annealing temperature of 800 °C of our setup. Under this condition, the slight colour changes (from red-orange to red-violet) for this system annealed above 700 °C can be entirely associated with surface and interface roughness changes taking place separately in both films, stimulated by thermally enhanced material diffusion.

On the contrary, for the Al_2O_3/ZnO system the solid state reaction in the applied temperature range is already known [2,6,7]. It allows us to assume a direct connection between the ORM spectra and the solid-state reaction process in the Al_2O_3/ZnO system. Furthermore, as an argument for the fact that the substrate material plays a minor role in the temperature-initiated ORM-colour changes, we performed additional ORM investigations of annealed Al_2O_3/ZnO samples grown on Si_3N_4 substrates. These studies showed that the colour palette for the samples grown on Si_3N_4 - although differing from that of the same films grown on SiO_2 substrate (probably due to a different refraction index of silicon nitride) – clearly shows strong temperature-dependent ORM-colour variations. We also performed separate studies of single Al_2O_3 and ZnO films on SiO_2 substrates. We found that an Al_2O_3 film does not reveal any colour change within the whole range of investigated temperatures, whereas the ZnO film reveales the same behaviour up to 700 °C. Only at 800°C noticeable colour changes were observed in the ZnO film presumably originating from strong recrystallization effects. That allows us to assume that the strong colour changes taking place in Al_2O_3/ZnO multilayer samples after annealing up to 700 °C are mainly driven by a solid state reaction process.

In order to track the formation of Kirkendall pores X-ray reflectivity (XRR) was applied. The XRR spectra of the as-grown and annealed Al_2O_3/ZnO samples grown on Si_3N_4 are presented in Fig. 3. It is obvious that for as-grown samples the signals from the Al_2O_3 and ZnO layers are strongly supressed. Only the thickness oscillations from the 100 nm thick Si_3N_4 substrate can be resolved. Relative to the

as-grown state, the sample annealed at 400 °C reveals only slight intensity variations without any additional features. At increased annealing temperatures between 500 °C and 800 °C the corresponding XRR-spectra undergo noticeable changes. To begin with, it is visible that between annealing temperatures of 500 °C and 700 °C an additional long-period oscillation can be detected at high incidence angles (marked with red arrows in Fig. 3). This oscillation can be associated with a thin layer forming in the multilayer structure. By means of annealing up to 700 °C this oscillation shifts towards lower theta angles. At 800 °C no signal of the corresponding layer structure can be detected. Secondly, by starting at 700 °C, other short-periodic oscillations can be detected at low theta angles. These oscillations become mostly pronounced at 800 °C when the long-periodic signal disappears.

The bright-field cross-section TEM micrographs made on Al_2O_3/ZnO systems in the as-grown state and after annealing at 600 °C for one hour are shown in Figs. 4(a) and 4(b), correspondingly. In the as-grown sample the Al_2O_3 and ZnO layers can be clearly identified. Both are amorphous and possess pronounced surface roughness. The surface of the amorphous Si_3N_4 buffer is, on the contrary, noticeably flat. No additional phases can be observed on the Al_2O_3/ZnO interface. This result correlates well with the XRR-data for the corresponding sample. After annealing at 600 °C strong changes take place within the whole system. Firstly, the roughness of the amorphous Al_2O_3 layer has been significantly lowered. Secondly, a crystallization of the ZnO layer takes place that reveals a typical contrast pattern with dominating grain diffraction phenomena. Finally, it is possible to resolve distinct additional contrast variations on the interface between the Al_2O_3 and ZnO films. This interfacial region is shown in Fig. 4(c) with increased magnification. Here, a new dark rough polycrystalline layer sharing its upper interface with the Al_2O_3 film is noticeable. Below this layer a thin bright line can also be distinguished which can be associated with material having much lower density than the surrounding layers. Taking into account that in the Al_2O_3/ZnO system a strong Kirkendall effect occurs between 500 °C and 700 °C [2], we assume that for the 600 °C-sample the observed interfacial features correspond to the SSR with a Kirkendall effect. So both new layers can be correspondingly associated with a $ZnAl_2O_4$ spinel layer and a layer with high void (pore) concentration. The reaction layer with corresponding stoichiometry at the interface between the Al_2O_3

and ZnO films was also identified by EDX measurements. The corresponding data are shown in Fig. 4(d).

The XRR spectrum of the 600°C-sample was fitted using a recursive Parrat algorithm [9]. For this purpose the software developed by Andreas Stierle, equipped with a root-mean square-deviation (χ^2) minimization algorithm for a precise numeric fitting procedure, has been applied in the present work [10]. The best fitting curve together with a corresponding electron density distribution model is presented in Fig. 5. Here, starting from the sample surface, XRR senses the dense 49 nm thick film, a 3 nm thin layer with an order of magnitude lower electron density, and a 100 nm thick Si_3N_4 substrate layer. According to the TEM image of the structure (Fig. 4) the layers detected by XRR can be correspondingly identified with an Al_2O_3 layer and a layer with Kirkendall pores. It is interesting that the XRR-model does not require any information about the 15 nm thick polycrystalline spinel layer as well as about polycrystalline 60 nm thick ZnO. The reason for this might be a high roughness of the corresponding films. This high roughness presumably dumps the XRR-oscillations from the corresponding layers making them irresolvable in the XRR spectrum. Obviously, the porous layer also possesses a high roughness. But the reason why the porous layer is nevertheless visible on the XRR-spectrum is assumed to be its higher optical contrast relative to the surrounding films.

Based on the extracted XRR-model we can deduce that the detected long-periodic oscillations in the XRR-spectra for samples annealed at 500 °C, 600 °C and 700 °C can be directly associated with the porous layer formed during the Kirkendall reaction. The shift of these oscillations towards lower theta values at high annealing temperatures can then be associated with increased thickness of the porous layer. Furthermore, the additional short-periodic oscillations at 700 °C up to 800 °C can be associated with the end phase of the SSR between Al_2O_3 and ZnO, i.e. the $ZnAl_2O_4$ spinel layer (≈60 nm thick), which has completely consumed the Al_2O_3 film. The fine structure of the XRR-oscillations at 800 °C reveals the increased interfacial quality of the spinel film. The disappearance of the oscillations from porous layers at 800 °C can be assigned to a re-crystallisation process in the spinel film. At this

temperature the voids are removed from the structure by enhanced diffusion processes, what had already been shown in previous studies [6,7].

Results and discussion

SSR in the Fe_2O_3/ZnO system

In the Fe_2O_3/ZnO system the composition of both contributing oxide layers made from ALD have been securely identified [11, 2]. Using GIXRD measurements we found that the as-grown Fe_2O_3 film is already polycrystalline which might initiate a crystallization process in the underlying as-grown amorphous ZnO film. This fact implies that the temperature-driven diffusion processes taking place in the Fe_2O_3/ZnO system might strongly differ from mechanisms previously proposed for the Al_2O_3/ZnO system, where the glass-like (amorphous) nature of the alumina determines the spinel-formation process. Nevertheless, similar to Al_2O_3/ZnO, for Fe_2O_3/ZnO we also expect a temperature-driven solid state reaction which should end up with the Franklinite spinel phase $ZnFe_2O_4$.

In Fig. 2 the ORM data for a Fe_2O_3/ZnO pair on 250 nm thick SiO_2 buffer demonstrate a temperature-initiated surface colour change between 600 °C and 700 °C. It points to a SSR between Fe_2O_3 and ZnO taking place in the mentioned temperature range.

The XRR-spectra for Fe_2O_3/ZnO samples annealed at 600 °C and 700 °C are presented in Fig. 6. Similar to the Al_2O_3/ZnO system, here the long-periodic oscillation maximum can be detected for the 600 °C-sample which shifts towards lower angles for the 700°C-sample. Taking the Al_2O_3/ZnO system as reference we identify the corresponding signals with a porous layer which is getting thicker with increasing annealing temperatures. Similar to the Al_2O_3/ZnO system, there are also short-periodic XRR-oscillations visible for the 600 °C-samples and disappearing at 700 °C – which can be identified as a thick spinel layer becoming rougher at 700 °C (probably due to a recrystallization process).

The GIXRD-data for 600 °C- and 700 °C-samples shown in Fig. 7 also clearly prove the presence of the stoichiometric $ZnFe_2O_4$ phase without any additional products [12].The transition from the non-

ferromagnetic as-grown Fe_2O_3/ZnO system to the ferromagnetic $ZnFe_2O_4$ spinel [13] after annealing at high temperatures was also confirmed by the SQUID magnetometry data (see Fig. 7). Interestingly, the data for the in-plane magnetization of the 700 °C-sample reveal the specific saturation magnetization of ≈350 emu/cm^{-3}, which points to the strong ferromagnetic properties of the formed zinc ferrite.

The cross-sectional TEM and STEM data for the Fe_2O_3/ZnO samples annealed at 600°C and 700°C for one hour with corresponding EDX-maps of the constituent materials are shown in Fig. 8. Here it is clearly visible that already after one hour annealing at 600 °C the whole Fe_2O_3 film is consumed and a polycrystalline thick "alloy" is formed. According to standard-free (semiquantitative) EDX quantification the Fe:Zn ratio of this "alloy" is close to 2:1 which points to the formation of the stoichiometric $ZnFe_2O_4$ spinel phase. One can also clearly resolve the nanometer-scale voids entering the remaining thin ZnO film at 600 °C, which coalesce to larger voids at 700 °C. The recrystallization process taking place in the system at 700 °C (see Fig. 6) can also be directly confirmed by the TEM data.

We state that the data from our indirect analyses (ORM, XRR, GIXRD, SQUID) are well consistent with the direct TEM and STEM/EDX observations. This allows us to conclude that in the Fe_2O_3/ZnO system a solid-state reaction accompanied by the Kirkendall effect takes place starting at 600 °C.

SSR in the Co_XO_Y/ZnO system

The final composition of the Co oxide produced using ALD is still a matter of discussions and assumptions in the scientific literature [14]. The situation is complicated because of the fact that in the as-grown state we found our Co oxide films to be amorphous, which makes it impossible to precisely analyse the phase and to identify the oxidation state using X-ray diffraction. Taking into account the fact that the ALD processes that we apply for Co oxide growth employ ozone as an oxidant, we assume that - similar to Fe_2O_3 - the end product of the cobalt oxide film should approach the highest oxidation state of the cobalt ions, i.e. the Co_2O_3 phase. Indeed, the GIXRD study of the Co_XO_Y system

annealed at 700 °C for one hour revealed the presence of a mixture of Co_2O_3 and CoO phases that offers some possibilities for a SSR in the Co_XO_Y/ZnO system.

In Fig. 2 the temperature-dependent ORM data for the Co_XO_Y/ZnO system are presented. It is possible to clearly resolve strong colour changes pointing to a SSR beginning approximately at 600 °C. In addition, the XRR-data in Fig. 9 reveal the morphologically distorted structure for the 600 °C-sample and a formation of a rough thin layer at 700 °C. Similar to the cases described above, this layer might be interpreted as a layer of pores.

A cross-section TEM image of the 700 °C-sample is shown in Fig. 10. It reveals the presence of a single substance presumably being a rough polycrystalline mixture of the constituent materials. On the GIXRD spectrum for the corresponding sample shown in Fig. 11 we identify three different phases: a CoO phase, a hexagonal (wurtzite) ZnO phase, and a phase close to stoichiometric $ZnCo_2O_4$. The CoO phase can be clearly identified by two characteristic peaks at 42.6° and 61.4°. In order to confirm our identification of the ZnO and spinel phases, the highly resolved part of the GIXRD spectrum between 29 and 40° is separately presented in Fig. 11 for pure ZnO and pure Co_XO_Y films as well as for the Co_XO_Y /ZnO sample annealed at 700 °C for one hour. Here it is possible to see that the peak at 32° on the spectrum from the Co-Zn-O film corresponds to a polycrystalline (100) ZnO reflection. The peak at 36.65° can be identified by comparing the experimental spectrum with tabular data for a bulk $ZnCo_2O_4$ phase [15] shown in Fig. 11. The experimental peak is close to the strongest reflection of the bulk spinel (36.96°). Furthermore, the spectrum in Fig. 11 for the annealed Co_XO_Y film reveals two peaks which can be associated with a Co_2O_3 phase. For the Co-Zn-O film one of these peaks disappears pointing to the transformation of the pure Co_2O_3 spinel into the Co-Zn-O spinel. The magnetic data in Fig. 12 do not reveal any ferromagnetism (FM), neither in the as-grown nor in the annealed samples. In the literature it is assumed that the presence of ferromagnetism in the $ZnCo_2O_4$ spinel is strongly determined by the presence of specific dopants: the n-type and neutral $ZnCo_2O_4$ phases are known to be anti-ferromagnetic, whereas the p-type phase shows a ferromagnetic response [16]. This allows us to assume that in our case an n-type doped cobalt-zinc spinel is formed at 700 °C.

The STEM/EDX mapping of the 700 °C-sample shown in Fig. 10 reveals the presence of two distinct phases: the Co-rich grains with correspondingly weaker Zn content and a Zn-rich residual phase with low Co content. According to our GIXRD data we correspondingly associate both phases with a $ZnCo_2O_4$ spinel and a remaining ZnO layer mixed with some CoO.

On the contrary to the XRR-data, the TEM observations of the 700 °C-sample do not reveal any evidence of voids. On the other hand, the TEM data in Fig. 10 reveal a clearly visible thin film at the interface with the SiO_2 substrate. EDX studies have shown that the corresponding layer is composed of a Zn-Si-O mixture probably being a result of temperature-driven interdiffusion of Zn atoms into SiO_2. So we conclude that for the Co_XO_Y/ZnO system the XRR-data for the 700 °C-sample actually reveal the formation of this interdiffusion-related Zn-Si-O layer but not the presence of a porous layer.

By taking all data into consideration we summarise that for the ALD-grown Co_XO_Y/ZnO system the presence of a SSR with the formation of a $ZnCo_2O_4$ spinel can be approved. Furthermore, the presence of an additional CoO phase as a result of high-temperature annealing of Co oxide is assumed to act as an n-type dopant being responsible for the non-ferromagnetic behaviour of the cobalt zinc spinel. The SSR in the Co_XO_Y/ZnO system is found to be not accompanied by a Kirkendall effect.

Conclusions

In the presented study we have investigated the temperature-dependent solid-state reactions and the Kirkendall effect in thin oxide film pairs grown using ALD. The results of our studies are summarized in Table 1, where the possibilities for the investigated systems to build complex spinel compounds at high temperatures as well as the possibility for the Kirkendall effect are shown. On an example of the ALD-grown Al_2O_3/ZnO thin film system we demonstrated the effectiveness of employing the large number of analysis methods to securely identify the solid-state reaction as well as to track and to study the Kirkendall effect. Using our methodology we found solid-state reactions in ALD-grown Fe_2O_3/ZnO and Co_XO_Y/ZnO thin film pairs. For the first time we report on the Kirkendall effect in the Fe_2O_3/ZnO system during a $ZnFe_2O_4$ spinel formation at temperatures between 600 °C and 700 °C. Furthermore, we report a strong ferromagnetism in the produced zinc ferrite structure. On the other hand, in the Co_XO_Y/ZnO system the SSR taking place at 700 °C proceeds without any evidence for the Kirkendall effect as well as without any evidence for ferromagnetism.

Acknowledgments

Work is supported by Deutsche Forschungsgemeinschaft (DFG) via Projects NI 616/11-1 (Hamburg) and HE 2100/8-1 (Halle).

List of tables

Table 1: Summary of the investigated systems. For each system the presence of a solid-state reaction as well as a Kirkendall effect are separately concluded. Ferromagnetism of the complex spinel after thermal annealing is also shown as a separate property of the investigated systems.

	Al_2O_3/ ZnO	Fe_2O_3/ ZnO	Co_XO_Y/ ZnO
SSR	yes	yes	yes
Kirkendall	yes	yes	no
Ferromagnetism of the final spinel	-	yes	no

List of figures

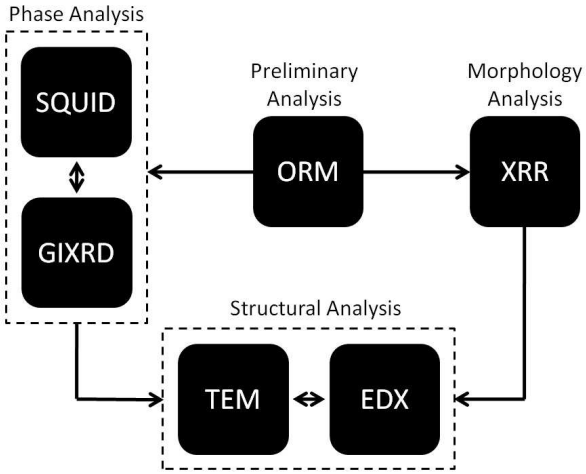

Figure 1: Flow-diagram describing the applied experimental procedure.

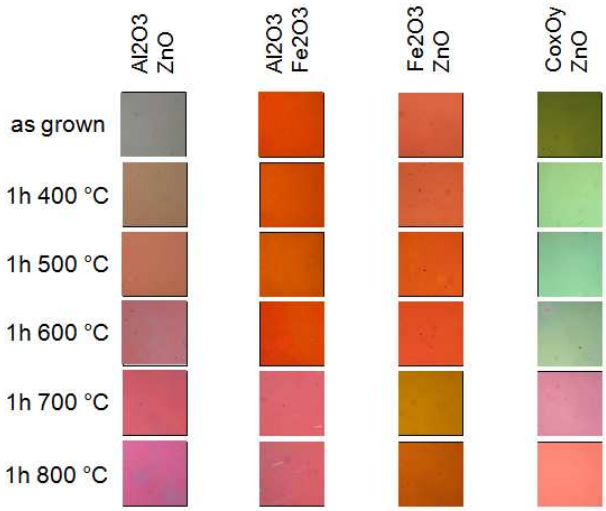

Figure 2: Optical reflection microscopy images of Al_2O_3/ZnO, Al_2O_3/Fe_2O_3, Fe_2O_3/ZnO, and Co_XO_Y/ZnO oxide thin film systems in their as-grown state and after one hour annealing at different temperatures. The image magnification is *x*10.

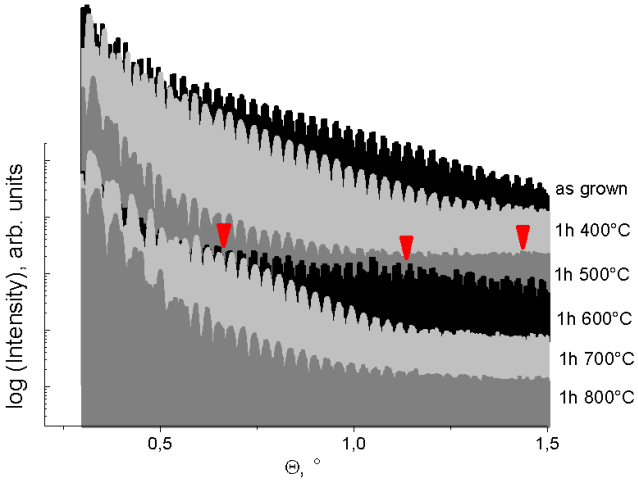

Figure 3: X-Ray reflectivity spectra of an Al_2O_3/ZnO /Si_3N_4(100nm)/Si(100) thin film system in its as grown state and after one hour annealing between 400 °C and 800 °C. The positions of long-periodic oscillations appearing between 500 °C and 700 °C are marked by red arrows.

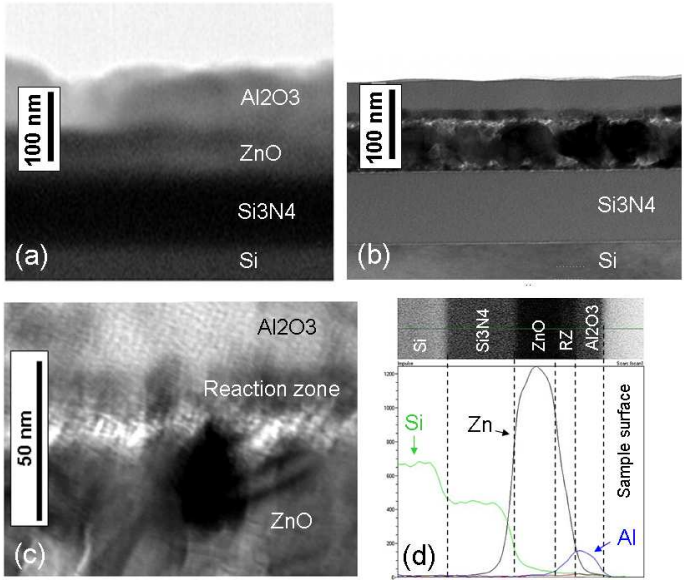

Figure 4: Cross-section TEM images of an Al_2O_3/ZnO system on Si_3N_4 (100 nm)/Si substrate (a) in its as-grown state, and (b) after one hour annealing at 600 °C. (c) Magnified image of the interaction area for the annealed sample, (d) EDX line scan for the main elements (Si, Zn, Al) along the vertical structure profile. “RZ” defines the reaction zone where Al_2ZnO_4 spinel formation takes place.

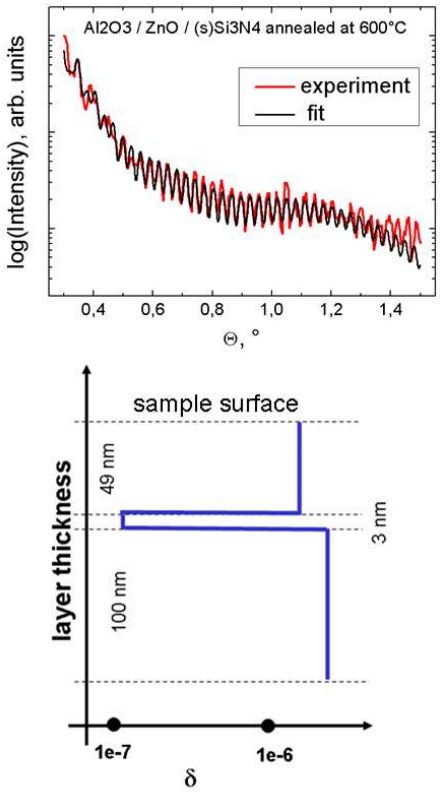

Figure 5: Experimental XRR-spectrum for the Al_2O_3/ZnO system on Si_3N_4(100 nm)/Si(100) after one hour annealing at 600 °C fitted by the spectrum for the model structure presented below. In the structure model δ is the real increment of the refractive index of the materials which is related to the material density.

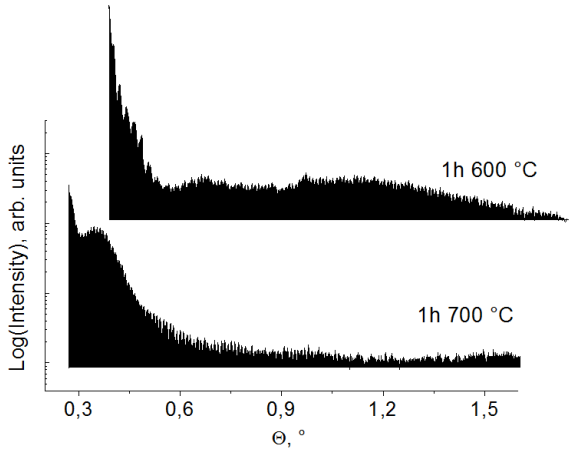

Figure 6: XRR-spectra of the Fe_2O_3/ZnO thin film system on SiO_2/Si(001) substrate after one hour annealing at 600 °C and 700 °C, respectively.

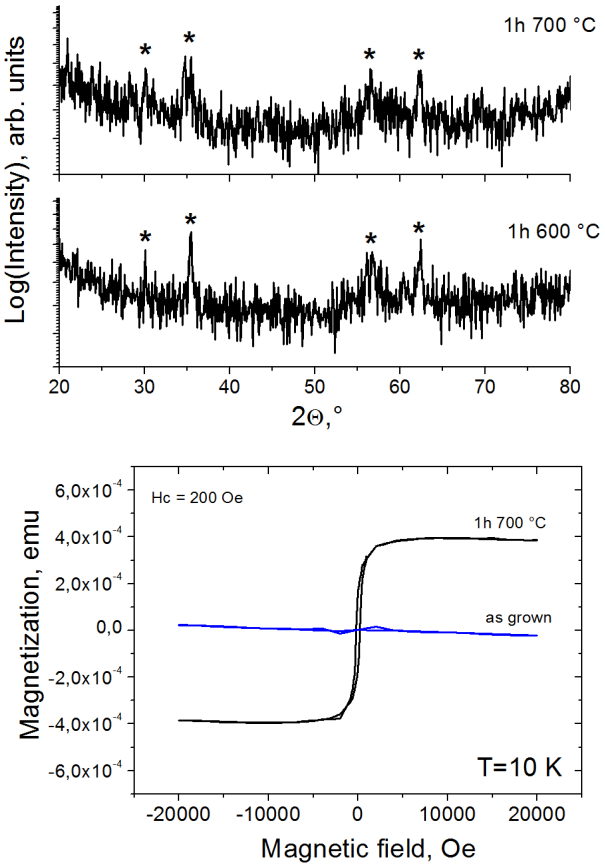

Figure 7: (above) GIXRD spectra for the Fe_2O_3/ZnO system on SiO_2/Si substrate after one hour annealing at 600 °C and 700 °C, respectively. The spectrum is rescaled for the CuKα wavelength. All visible peaks (marked with asterisks) can be identified with a $ZnFe_2O_4$ phase with lattice constant of 0.837 nm (a_{bulk}=0.841 nm); (below) Magnetization data for the Fe_2O_3/ZnO system in as-grown and annealed states (700 °C; 1h) measured at 10K. The ferromagnetism in the annealed sample can be related to the formation of the magnetic spinel phase.

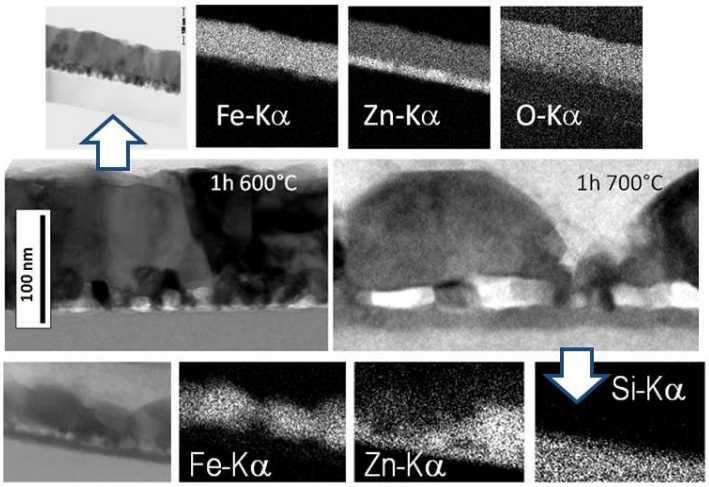

Figure 8: Cross-section TEM and STEM images of the Fe_2O_3/ZnO system on SiO_2/Si substrate after one hour annealing at 600 °C and 700 °C, respectively. The corresponding elementary EDX maps of cross-sections clearly show the presence of the formed Fe-Zn-O phase. It is possible to resolve the thin porous layer for the 600 °C sample, whereas for the 700 °C sample transformations into larger agglomerated pores results, and a recrystallization of the $ZnFe_2O_4$ phase takes place.

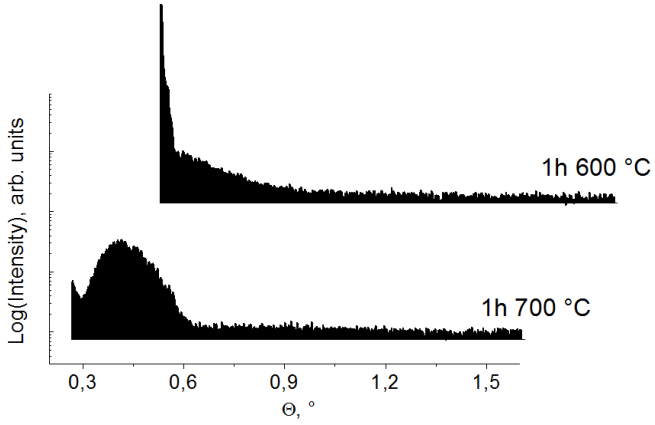

Figure 9: XRR-spectra of the Co_XO_Y/ZnO thin film system on SiO_2/Si(001) substrate after one hour annealing at 600 °C and 700 °C.

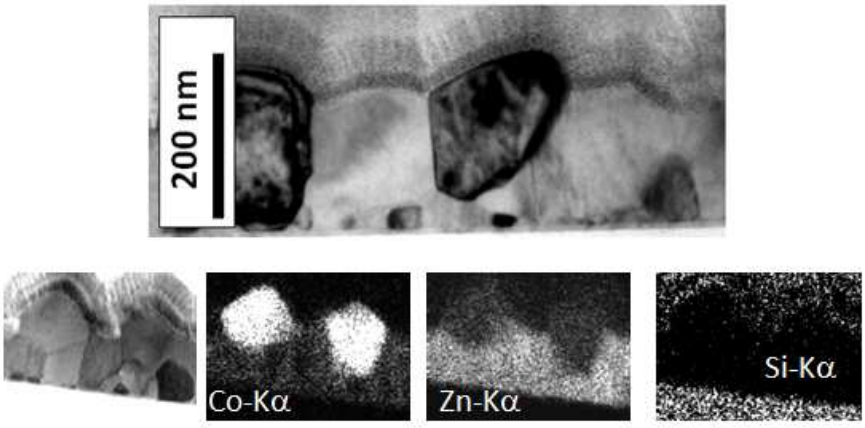

Figure 10: Cross-section TEM and STEM images of a Co_XO_Y/ZnO sample on SiO_2/Si substrate after one hour annealing at 700 °C. The elementary EDX maps of the cross section reveal the intermixing of Zn and Co atoms forming two different phases: the Co-rich and the Zn-rich one. The fine-crystalline contrast layer above the large crystallites is a thinning artifact (sputtered from the sample during the ion-beam thinning process and re-deposited on the actual sample surface, see EDX spectrum for the Si-distribution).

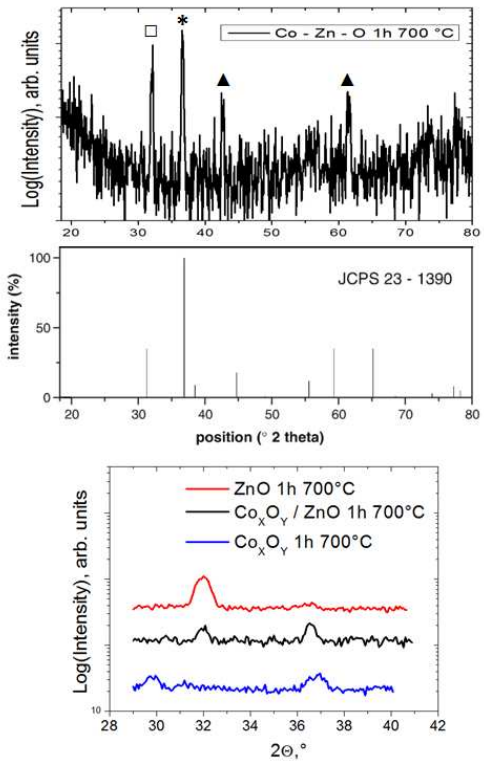

Figure 11: (Above) GIXRD spectra of the Co_XO_Y/ZnO system on SiO_2/Si substrate after one hour annealing at 700 °C compared to the database spectrum of polycrystalline $ZnCo_2O_4$ spinel. The spectrum is rescaled for the CuKα wavelength. The experimental diffraction peaks are identified as following: (square) – wurtzite (100) ZnO, (asterisk) – (311) $ZnCo_2O_4$ spinel, (triangle) – (200) and (220) cubic CoO. (Below) Part of the experimental GIXRD spectra for pure ZnO, Co_XO_Y films annealed for one hour at 700 °C, compared with the spectrum from the annealed Co_XO_Y/ZnO system.

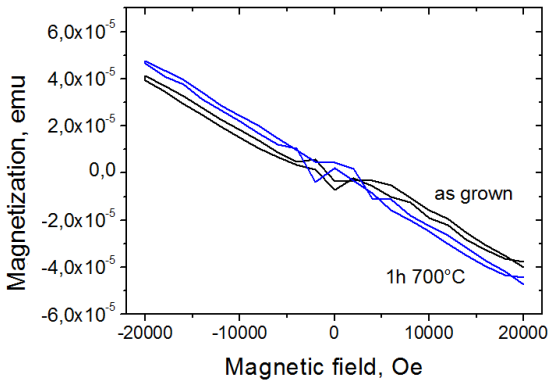

Figure 12: Magnetization data taken at 10K for Co_XO_Y/ZnO samples in as-grown and annealed states (700 °C; 1h). The curves show the absence of resolvable ferro- and paramagnentism in both samples. The observed diamagnetism stems from the sample holder. The property of the annealed sample can be tentatively associated with the n-type $ZnCo_2O_4$ spinel.

References

[1] Yadong Yin, Robert M. Rioux, Can K. Erdonmez, Steven Hughes,Gabor A. Somorjai, A. Paul Alivisatos, *Science* **2004**, 304, 711

[2] H.J.Fan, M.Knez. R. Scholz, K. Nielsch, E. Pippel, D. Hesse, M. Zacharias, U. Gösele, *Nature Materials* **2006**, 5, 627

[3] A. D. Smigelskas, E. O. Kirkendall, *Trans. AIME* **1947**, 171, 130

[4] Riikka L. Puurunen, *J. Appl. Phys.* **2005**, 97, 121301

[5] M. Knez, K. Nielsch, and L. Niinistö, *Adv. Mater.* **2007**, 19, 3425

[6] Y. Yang, D. S. Kim, R. Scholz, M. Knez, S. Mo Lee, U. Gösele, and M. Zacharias, *Chem. Mater.* **2008**, 20, 3487

[7] H.J. Fan, M. Knez, R. Scholz, D. Hesse, K. Nielsch, M. Zacharias, and U. Gösele, *Nano Letters* **2007**, 7, 993

[8] Lisa A. Tietz, and C. Barry Carter, *J. Am. Ceram. Soc.* **1992**, 75, 151 1097

[9] L. G. Parrat, *Phys. Rev. B* **1954**, 95, 359

[10] The information about program “fewlay” can be obtained from Andreas Stierle (stierle@mf.mpg.de).

[11] Bachmann J., Jing J., Knez M., Barth S., Shen H., Mathur S., Gosele U., Nielsch K., *J. Amer. Chem. Soc.* **2007**, 129, 9554

[12] Sesha S. Srinivasan, Jeremy Wade, and Elias K. Stefanakos, *J. Nanomat.* **2006**, Article ID 45712

[13] H. H. Hamdeh, J. C. Ho, S. A. Oliver, R. J. Willey, G. Oliveri, G. Busca, *J. Appl. Phys.* **1997**, 81, 1851.

[14] Riikka L. Puurunen, *J. Appl. Phys.* **2005**, 97, 121301

[15] K. Karthikeyan, D. Kalpana, N. G. Renganatan, Syntheis and characterization of ZnCo2O4 nanomaterial for symmetric supercapacitor applications, Ionics, Spinger-Verlag **2008**.

[16] H. J. Kim, I. C. Song, J. Ho Sim, H. Kim, D. Kim, Y. Eon Ihm, and W. Kil Choo, *phys. stat. sol.* **2004**, 241, 1553